Integrated optomechanical analysis of adaptive optical systems

Keith B. Doyle, Victor L. Genberg, Gregory J. Michels
Sigmadyne, Inc.
803 West Avenue, Rochester, NY

ABSTRACT

A method to predict performance of adaptive optical systems subject to mechanical perturbations is presented. Integrated modeling techniques coupling finite element analysis and optical design software are discussed that enable mechanical design trades of an adaptive mirror assembly based on correctability of the optical system wavefront error. This method is based on the linearity of wavefront error consistent with that caused by mechanical disturbances during operation. Optical surface sensitivities are computed based on rigid-body and higher-order surface deformations that relate mechanical surface errors to optical system wavefront error. The sensitivities are then used to determine the best-fit set of actuators to minimize the wavefront error in the optical system due to finite element derived mechanical disturbances. An example is demonstrated for a Cassegrain telescope with an active primary mirror.

Keywords: Integrated modeling, deformable mirrors, finite element analysis, active optics

1. INTRODUCTION

The integration of optical system design tools including thermal, structural, and optical analyses enables high-performance optical systems, such as adaptive optical systems, to be designed and built for optimum performance. In an adaptive optical system, image motion and wavefront error are reduced by moving and deforming one or more optical surfaces. Many mechanical design variables must be taken into consideration when optimizing an adaptive mirror assembly such as number of actuators, actuator spacing, and facesheet thickness such that the deformable mirror may be actuated to best correct the aberrations present in the optical system. Use of optimization techniques in the design of adaptive components is discussed by Michels[1]. Integrating thermal, structural, and optical design tools has been enhanced by the development of interfacing software such as the optomechanical analysis program *SigFit*[2] to allow efficient coupling between the industry standard tools. In extending this capability to the analysis of adaptive systems, parametric design trades of the adaptive assembly may be performed as a function of overall optical system performance.

2. COMPONENT ADAPTIVE ANALYSIS

Traditionally, in the mechanical design and analysis of an adaptive component, the set of actuator forces or displacements are determined that minimizes the surface error of the adaptive mirror. Correcting Zernike surface errors such as power, astigmatism, coma, and trefoil are investigated as measures of the adaptive mirror's ability to remove the corresponding wavefront error in the optical system. In addition, the adaptive mirror's ability to correct environmental influences such as gravity, mount strain, and thermal gradients are also evaluated. Once actuator inputs have been found, the residual-surface error, correctability, and other performance metrics may be computed. Correcting the surface error of a hexagonal segment using force and displacement actuators is illustrated in Figure 2.1. The corrected surface is equal to the sum of the uncorrected deformed surface plus each of the actuator influence functions scaled by each actuator's

respective actuator input as depicted schematically in Figure 2.2[3]. This analysis may be extended to segmented surfaces as shown in Figure 2.3[4].

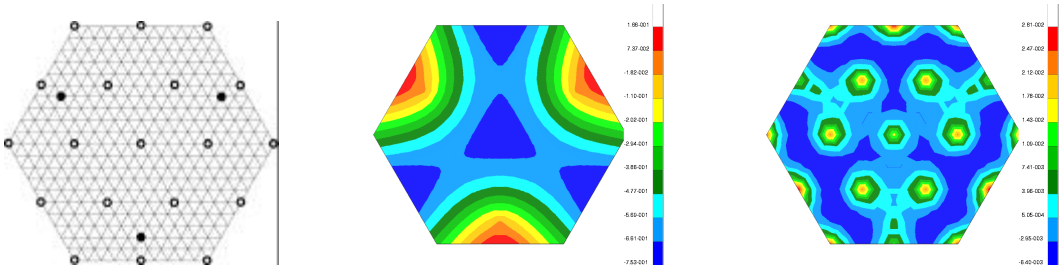

(a) (b) 0.510 λ's rms (c) 0.006 λ's rms

Figure 2.1 Surface analysis example; a) Finite element model of a hexagonal mirror segment - solid circles indicate displacement actuator locations, while open circles indicate force actuator locations; b) uncorrected surface deformation due to gravity, and c) the corrected surface.

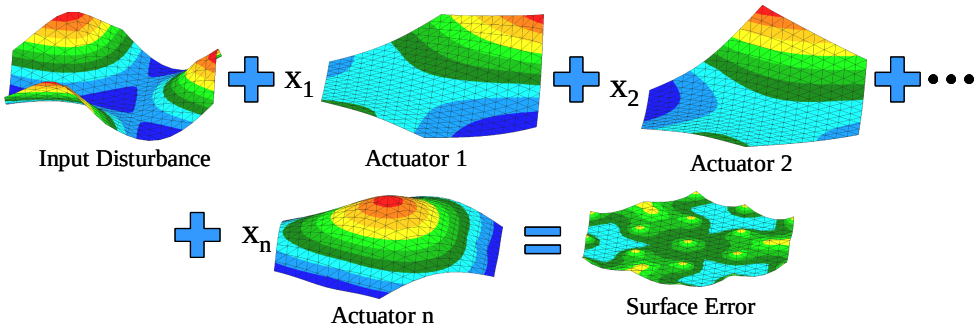

Figure 2.2 Illustration of adaptive control simulation. The unactuated deformed surface plus all of the influence functions scaled by the actuator inputs equals the corrected surface.

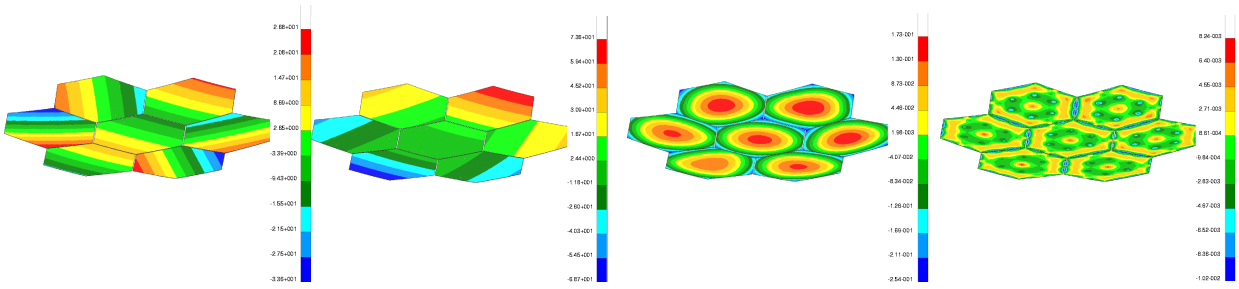

(a) (b) (c) (d)

Figure 2.3 Segmented mirror example; a) Finite element model of a seven segment mirror showing uncorrected surface error of 28 μm; b) surface error of 11.1 μm after array rigid-body correction motion; c) surface error 0.09 μm after segment rigid-body correction of; and d) surface error of 0.003 μm after segment rigid-body and surface correction.

Mathematically, adaptive simulation is achieved by minimizing the mean square surface error of the perturbed optical surface. The corrected displacement of the *i*th node, ds_i^{Corr}, is the sum of the uncorrected displacement of the *i*th node, ds_i, and the sum of the displacements induced by each actuator,

$$ds_i^{Corr} = ds_i + \sum_j \mathbf{x}_j dx_{ji} \ , \tag{2.1}$$

where x_j is the variable actuator input for the *j*th actuator, and dx_{ji} is the displacement of the *i*th node for the *j*th actuator's influence function. The influence function for a particular actuator is the deformed surface due to a unit input of that actuator while all other inputs are zero. The mean square residual error, *E*, of the corrected optical surface is represented by the following relationship,

$$E = \sum_i w_i \left(ds_i + \sum_j x_j dx_{ji} \right)^2 \ , \tag{2.2}$$

where w_i is the area weighting of the *i*th node. (Area weighting is discussed in more detail by Genberg[5]).

The actuator inputs that minimize the mean square error, *E*, are found by taking derivatives of Eq. (2.2) with respect to each actuator input, x_j, and setting each resulting equation equal to zero. This results in the following linear system represented by Equ. (2.3):

$$[H]\{X\} = \{F\} \ , \tag{2.3}$$

where

$$H_{jk} = \sum_i w_i dx_{ji} dx_{ki} \ ,$$

and

$$F_k = \sum_i w_i ds_i dx_{ki} \ . \tag{2.4}$$

The adaptive mirror's residual surface error may be determined once the actuator inputs have been found from Equ. (2.4). The corrected surface may be represented in optical design tools using interferogram files (CODE V, OSLO) or as a Grid Sag surface in Zemax[6] to predict overall optical performance of the adaptive optical system.

3. INTEGRATED ADAPTIVE ANALYSIS

Mechanical design trades may be parametrically performed as a function of the correctability of the optical system by coupling the structural and optical design tools. This approach is based upon the method of superposition and the linearity of wavefront error. For the small surface

perturbations typical of adaptive optical systems, this approximation is generally valid. *SigFit* performs this computation by importing the change in the wavefront error of the optical system in the exit pupil due to each influence function and each environmental perturbation in consideration. The influence function for each actuator is computed using finite element analysis. This allows the forces and displacements of the actuators to be selected to minimize the wavefront error of the optical system based on a set of mechanical and thermal perturbations for each of the optical elements in the optical system. For example, the optimum actuation of the primary mirror of a telescope assembly may be selected such that distortions of the secondary mirror are corrected. This technique works for a single adaptive mirror in a telescope system, or with multiple adaptive mirrors. For example, an optical system may possess an adaptive primary and a secondary mirror with focus correction.

Optical system wavefront error sensitivities are computed by perturbing the deformable surface in the optical model. For force actuators, which produce a global displacement of the optical surface (Figure 3.1a), the influence function may be described using Zernike polynomials. In this case, wavefront error sensitivities are computed by perturbing the optical surface within the optical model a unit amount for each Zernike term. For displacement actuators, which produce a local displacement of the optical surface (Figure 3.1b) where an accurate Zernike fit may not be achieved, the deformed optical surface is represented by a uniform grid of data. The grid file is passed to the optical model where the effect on wavefront error in the exit pupil is computed and output as a uniform grid of data.

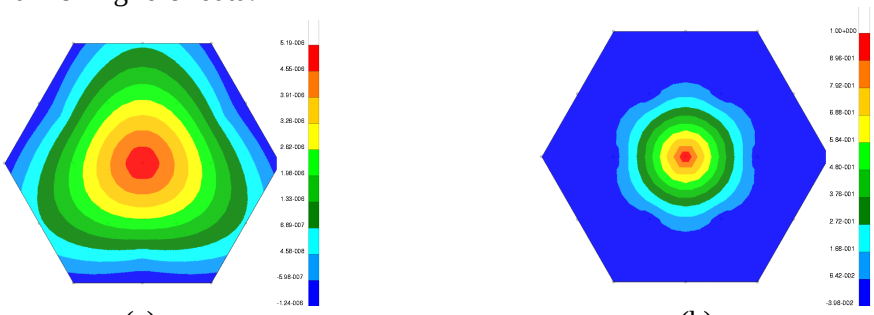

(a) (b)

Figure 3.1 Typical Influence functions: (a) global effect of force actuator (b) local effect of displacement actuator.

The mathematical description for performing integrated adaptive analysis using Zernike decomposition techniques is provided below[7]. For influence functions unable to be described accurately by Zernike polynomials then it is a simple extension in the programming to use grid interferogram files as input and output from the optical design code.

A sensitivity matrix, S_{kj}^{n}, represented by a set of Zernike terms, k, is computed from the optical system model by perturbing each optical surface, n, by a unit Zernike surface perturbation, j. The units of the sensitivity matrix are wavefront error in waves per surface deformation. The sensitivity matrix is used to convert each actuator influence function, F_{m}^{t}, where m is the actuator number and t is the adaptive surface, into a corresponding optical response in terms of wavefront error at the exit pupil (i.e. optical influence function), U_{km}^{n}.

This is achieved by decomposing each actuator influence function into Zernike coefficients, B_{jm}^{t}, and multiplying each term by the sensitivity matrix to yield the optical influence functions

$$U_{km}^{t} = S_{kj}^{t} B_{jm}^{t} \tag{3.1}$$

for each optical surface.

For a given perturbed state of the optical system due to an environmental load, each deformed surface is decomposed into Zernike coefficients, C_{ji}^{n}, where, *j*, is the vector of Zernike coefficients for load case, *i*, of each optical surface, *n*. The wavefront error of the optical system is computed by multiplying the optical sensitivities by the Zernike terms of the deformed surface:

$$Z_{ki} = \sum S_{kj}{}^{n} C_{ji}{}^{n} \tag{3.2}$$

where Z_{ki} is vector of Zernikes, *k*, for each load case, *i*.

Fitting the actuators to minimize the wavefront error is performed using a least-squares fit. A system error, *E*, is defined as:

$$E = \sum_{k}^{Z} w_k \left(Z_{ki} - \sum_{m}^{M} U_{km} A_m \right)^2 \tag{3.3}$$

where A_m is the contribution of each actuator. To compute the best-fit actuator coefficients, the error function is minimized with respect to the coefficients. This is performed by taking the derivative of the error function with respect to the coefficients and setting it equal to zero:

$$\frac{dE}{dA_q} = \sum_{k}^{Z} w_k 2 \left(Z_{ki} - \sum_{m}^{M} U_{km} A_m \right) U_{kq} = 0 \tag{3.4}$$

Rearranging terms yields the following expression:

$$\sum_{k}^{Z} w_k \left(\sum_{m}^{M} U_{km} U_{kq} A_m \right) = -\sum_{k}^{Z} w_k \left(Z_{ki} \right) U_{kq} \tag{3.5}$$

The actuator coefficients may be solved via the following matrix equation:

$$[H]\{A\} = \{F\} \tag{3.6}$$

where

$$H_{qm} = \sum_{k}^{Z} w_k U_{qk} U_{km} \tag{3.7}$$

and

$$F_q = -\sum_{k}^{Z} w_k Z_k U_{kq} . \tag{3.8}$$

The weighting of each Zernike term, w_k, may be specified as the surface RMS of one wave of Zernike, *k*, over a unit circle.

4. INTEGRATED ADAPTIVE ANALYSIS EXAMPLE

A Cassegrain telescope was used to demonstrate the above methodology and the validity of wavefront superposition. The telescope operating at a wavelength of 600 nm consists of a primary and secondary mirror as shown in the finite element and optical models in Figure 4.1.

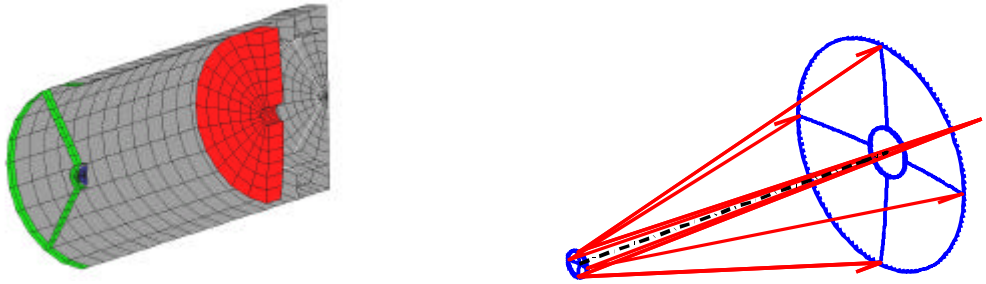

(a) (b)

Figure 4.1 Cassegrain telescope models; a) finite element model and b) optical model.

The active surface is the primary mirror consisting of nine force actuators and three displacement actuators whose location is shown in Figure 4.2. Each of the primary mirror's surface influence functions were fit to a set of Fringe Zernike polynomials. The primary and secondary mirror optical surface sensitivities were next computed. Rigid-body sensitivities were computed by applying a unit perturbation in each of the six degrees-of-freedom of the primary and secondary mirror and recording the wavefront error in the exit pupil as represented by Zernike polynomials. The higher-order optical surface sensitivities of the primary and secondary mirror were computed based on a unit wave of each of the Fringe Zernikes applied individually to each mirror's surface in the optical model. The resulting exit pupil wavefront error was subsequently fit to Fringe Zernike polynomials. A CODEV macro program was used to help automate the computation of the sensitivity maps.

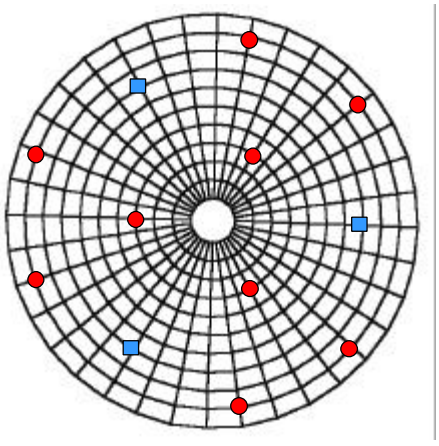

Figure 4.2 Active primary mirror with nine force actuators represented as circles and three displacement actuator represented as squares.

Optical system correctability was based upon the ability of the actuators on the primary mirror to correct surface errors of the primary and secondary mirrors. Gravity acted along the optical axis of the telescope creating 4.62 and 2.18 waves rms of surface error on the primary and secondary

mirrors, respectively. In addition, five waves of astigmatism was added to the surface distortion of the secondary mirror. The surface errors of the primary and secondary mirrors were separated into rigid-body errors and higher-order surface deformations. The higher-order surface displacements were fit to Fringe Zernike polynomials. Contour plots of the primary and secondary mirror surface errors along with the resulting optical system wavefront error of 11.25 waves rms is shown in Figure 4.3.

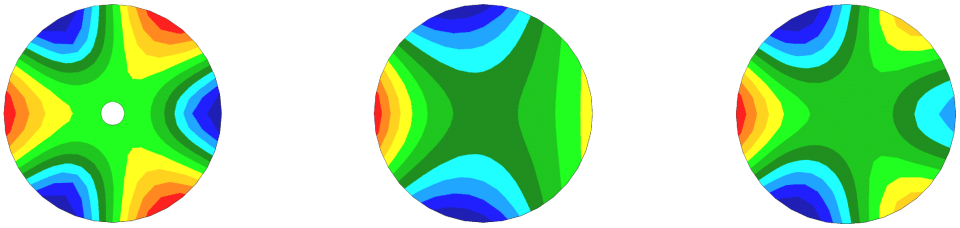

(a) (b) (c)

Figure 4.3 a) Primary mirror surface error of 4.62 waves rms; b) secondary mirror surface error of 2.18 waves rms; and c) resulting optical system wavefront error of 11.25 waves rms.

Traditional analyses determine the motion of the actuators that minimize the surface error of the adaptive surface – in this case the primary mirror. This analysis was performed and the results presented in Figure 4.4. The residual surface error in the primary mirror is 0.11 waves rms after correction by the actuators. However, optical system wavefront error is still significant at 4.31 waves rms due to the surface errors of the secondary mirror.

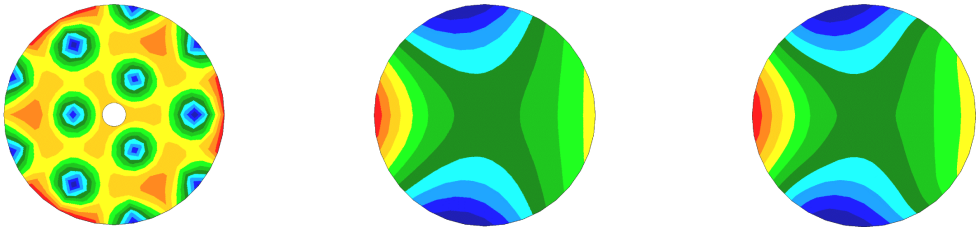

(a) (b) (c)

Figure 4.4 Primary mirror surface error correction results in a) primary mirror surface error of 0.11 waves rms; and leaves the b) the secondary mirror surface error of 2.18 waves rms uncorrected; c) and results in an optical system wavefront error of 4.31 waves rms.

A system level analysis was then performed using *SigFit* that deformed the primary mirror to the shape that minimized the wavefront error in the optical system. These results are shown in Figure 4.5. The contour plot of the primary mirror surface error is of the same shape but opposite sign of the secondary mirror. These optical surface errors combine to yield an overall optical system wavefront error of 0.23 waves rms.

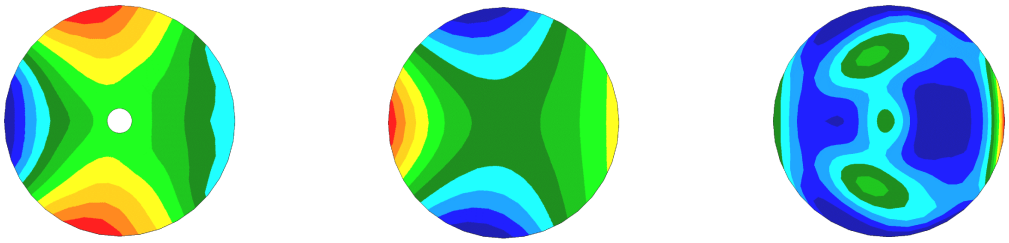

(a) (b) (c)

Figure 4.5 System wavefront error correction results in a) 2.18 waves rms surface error of the primary mirror that corrects b) the 2.18 waves rms surface error of the secondary mirror resulting in c) optical system wavefront error correction of 0.23 waves rms.

The above method assumes linearity of the wavefront error for small perturbations of the optical surfaces consistent with those of mechanical deformations. Validation was performed by creating surface interferogram files for both the primary and secondary surfaces for the uncorrected and the corrected systems and applying them to the CODEV optical model. Wavefront error maps computed by CODEV are shown for both the uncorrected and corrected systems in Figure 4.6. These match the SigFit computed wavefront error maps using the optical surface sensitivities. A more detailed comparison showing each of the Zernike terms for the uncorrected and corrected system is presented in Table 1. The Zernike coefficients for both techniques denoted by CODEV, for the interferogram file approach, and *SigFit*, using the superposition approach, are virtually identical.

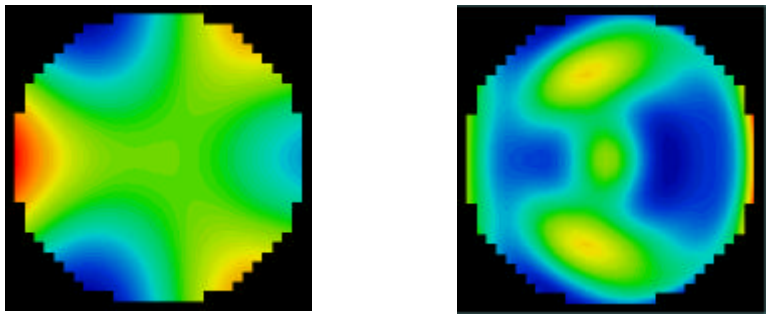

Figure 4.6 CODEV wavefront error maps of a) uncorrected system with 11.23 waves rms and b) corrected system with 0.22 waves rms.

SUMMARY

A method is presented that couples finite element and optical design software tools to allow the correctability of an adaptive optical system to be predicted based upon optical system wavefront error. This approach is based upon the method of superposition and the linearity of wavefront error consistent with small surface perturbations due to mechanical disturbances. Optical system wavefront error is related to mechanical surface errors via optical surface sensitivity maps. The surface sensitivity maps are computed by perturbing each optical surface a unit amount in six rigid-body degrees-of-freedom and higher-order surface deformations based on a unit Zernike perturbation for force actuators and individual influence functions for displacement actuators. The wavefront error is then recorded at the exit pupil of the optical system. This allows the forces and displacements of the actuators to be selected to minimize the wavefront error of the optical system based on a set of mechanical and thermal perturbations for each of the optical

elements in the optical system. This method was demonstrated on a Cassegrain telescope with an active primary mirror with primary and secondary mirror surface errors with the optomechanical analysis software *SigFit*. Validation was performed using the optical design software CODE V by using surface interferogram files to represent the perturbed and corrected optical surface deformations. Resultant wavefront error maps computed by *SigFit* and CODEV were shown to be virtually identical verifying wavefront linearity for the system demonstrated.

	No-Corr	No-Corr	Corr'd	Corr'd		No-Corr	No-Corr	Corr'd	Corr'd
ZFR	CodeV	SigFit	CodeV	SigFit	ZFR	CodeV	SigFit	CodeV	SigFit
2	-0.01	0.00	-0.01	0.00	21	0.00	0.00	-0.02	-0.02
3	0.00	0.00	0.00	0.00	22	0.00	0.00	0.00	0.00
4	-1.75	-1.75	0.01	0.00	23	0.00	0.00	-0.01	-0.01
5	9.91	9.91	0.04	0.04	24	0.00	0.00	0.00	0.00
6	0.00	0.00	0.00	0.00	25	-0.10	-0.10	0.11	0.11
7	0.00	0.00	0.24	0.24	26	0.00	0.00	0.09	0.09
8	0.00	0.00	0.00	0.00	27	0.00	0.00	0.00	0.00
9	1.85	1.85	0.00	0.00	28	0.00	0.00	0.01	0.01
10	-29.09	-29.10	0.00	0.00	29	0.00	0.00	0.00	0.00
11	0.00	0.00	0.00	0.00	30	-0.75	-0.76	0.22	0.22
12	-0.02	-0.02	0.57	0.57	31	0.00	0.00	0.00	0.00
13	0.00	0.00	0.00	0.00	32	0.00	0.00	0.01	0.01
14	0.00	0.00	-0.03	-0.03	33	0.00	0.00	0.00	0.00
15	0.00	0.00	0.00	0.00	34	0.00	0.00	0.00	0.00
16	-0.43	-0.43	0.00	0.00	35	0.00	0.00	0.00	0.00
17	0.00	0.00	0.16	0.16	36	-0.02	-0.02	-0.11	-0.11
18	0.00	0.00	0.00	0.00	37	0.10	0.10	0.07	0.07
19	5.18	5.19	-0.04	-0.04					
20	0.00	0.00	0.00	0.00	RMS	11.23	11.25	0.22	0.23

Table 1. Zernike comparison of corrected and uncorrected wavefront error results using SigFit's Zernike superposition and CODEV

REFERENCES

[1]Michels, G. J., Genberg, V. L., "Design optimization of actively controlled optics", *Proceeding of SPIE*, **4198**, Bellingham, WA (2000).

[2]SigFit is a product of Sigmadyne, Inc.

[3]Doyle, K. B., Genberg, V. L., Michels, G. J., "*Integrated Optomechanical Analysis*" SPIE Tutorial Text 58, (2002).

[4]Genberg, V. L., Michels, G. J., "Opto-mechanical analysis of segmented/adaptive optics", *Proceedings of SPIE*, **4444**, Bellingham, WA (2001).

[5]Genberg, V. L., Michels. G. J., Doyle, K. B., "Making Mechanical FEA Results Useful in Optical Design", SPIE(4769), July, 2002, Seattle, WA.

[6]Genberg, V. L., Michels, G. J., Doyle, K. B. "Orthogonality of Zernike Polynomials", *Proc. of SPIE*, 4771(33), Bellingham, WA, 2002.

[7]Genberg, V. L., Doyle, K.B., Michels, G.J., "Optical performance as a function of dynamic mechanical loading", SPIE AM03-412, 2003.